

## Modeling Substituent and Conformational Effects on the Reactivity of Antitumor Agents Containing a Cyclopropylcyclohexadienone Subunit

Mauro Freccero\* and Remo Gandolfi

Dipartimento di Chimica Organica, Università di Pavia, V.le Taramelli 10, 27100 Pavia Italy

freccero@unipv.it

Received May 13, 2004

The uncatalyzed alkylation reactions of ammonia by the parent spirocyclopropylcyclohexadienone (**6**), its 3-amino analogue (**7**), the cyclic derivative (**8**), its *N*-formyl derivative (**9**), and a closer model (**10**) of the CPI (**1–4**) drugs have been investigated in gas phase and in water solvent bulk, using density functional theory at the B3LYP level with several basis sets and the C-PCM solvation model. The effect of several structural key features such as the vinylogous amide conjugation, the acylation of the 2-amino substituent, the ring constraint of the heterocyclic nitrogen atom at C<sub>2</sub> carbon in a ring, and the presence of a condensed pyrrole ring on the reaction activation energy have been investigated. Substrate **7**, which is a flexible conformational model of the cyclopropylpyrroloindole moiety (CPI) contained in the duocarmycins, has been used to model the shape-dependent reactivity of these drugs, in gas phase and water solutions. The calculations indicate that shape dependence of reactivity is strongly operative both in gas phase and in polar solvents, since conformational effects are capable of reducing the reaction activation energy by  $-8.4$  and  $-4.3$  kcal mol<sup>-1</sup> in gas phase and in water solution, respectively, that is required to promote “conformational catalysis”.

### Introduction

The cyclopropylpyrroloindoles (CPIs) have received considerable attention as extremely potent DNA alkylating agents.<sup>1</sup> Exploitation of these agents as interstrand cross-linkers was originally reported by Mitchell,<sup>2</sup> and more recently a wide array of second-generation CPI dimers have been investigated with respect to both interstrand cross-linking and monoalkylation properties.<sup>3</sup> Among CPIs, of particular notoriety are the duocarmycins **1**, **2**, CC-1065 (**3**) (Scheme 1),<sup>4,5</sup> and very recently yatake-mycin (**4**).<sup>6</sup> The natural products and synthetic analogues containing the CPI or similar moieties (see the highlighted substructures in Scheme 1) are capable of se-

quence-selective alkylation of DNA at adenine N-3 center, within the DNA minor groove.<sup>7</sup> The formation of a covalent bond involving the unsubstituted cyclopropane carbon (C<sub>7</sub>) is the reaction mediating the potent biological effects of these drugs.

The reacting core of CPI drugs is the spirocyclopropylcyclohexadienone (**6**) moiety, which as pointed out previously by Winstein may be considered an homologue of the *p*-quinone methide (*p*-QM, **5**).<sup>8</sup> In fact **6** retains an electronic conjugation comparable to that of **5**, as shown by a similar UV spectrum,<sup>8b</sup> and it displays, like QMs, a general sensitivity to acid-catalyzed addition.<sup>9</sup> Furthermore, both undergo facile nucleophilic addition to affords homobenzylic and benzylic adducts, respectively (see Scheme 2). Notwithstanding such similarities the “cyclopropyl quinone methide” **6** (according to Winstein’s definition)<sup>8a</sup> is generally more resistant to a nucleophilic attack in comparison to **5** and displays a lower sensitivity to acid-catalyzed solvolysis. In fact, it is well-known from experimental<sup>10,11</sup> and computational data<sup>12</sup> that H-bonding with both protic solvents and substrates enhances the electrophilicity of QMs such as **5** and its *ortho* isomer.

\* To whom correspondence should be addressed. Tel: +39 0382 507668. Fax: +39 0382 507323.

(1) (a) Boger, D. L.; Johnson, D. S. *Angew. Chem., Int. Ed. Engl.* **1996**, *35*, 1438. (b) Boger, D. L.; Boyce, C. W.; Garbaccio, R. M.; Goldberg, J. *Chem. Rev.* **1997**, *97*, 787. (c) Boger, D. L. *Acc. Chem. Res.* **1995**, *28*, 20. (d) Rajsiki, S. R.; Williams, R. M. *Chem. Rev.* **1998**, *98*, 2723. (e) Wolkenberg, S. E.; Boger, D. L. *Chem. Rev.* **2002**, *102*, 2477.

(2) (a) Mitchell, M. A.; Kelly, R. C.; Wicnienski, N. A.; Hatzenbuehler, N. T.; Williams, M. G.; Petzold, G. L.; Slightom, J. L.; Siemieniak, D. R. *J. Am. Chem. Soc.* **1991**, *113*, 8994. (b) Mitchell, M. A.; Johnson, P. D.; Williams, M. G.; Aristoff, P. A. *J. Am. Chem. Soc.* **1989**, *111*, 6428.

(3) (a) Seaman, F. C.; Chu, J.; Hurley, L. *J. Am. Chem. Soc.* **1996**, *118*, 5383. (b) Lee, S. J.; Seaman, F. C.; Sun, D.; Xiong, H.; Kelly, R. C.; Hurley, L. H. *J. Am. Chem. Soc.* **1997**, *119*, 3434.

(4) (a) Takahashi, I.; Takahashi, K.; Ichimura, M.; Morimoto, M.; Asano, K.; Kawamoto, I.; Tomita, F.; Nakano, H. *J. Antibiot.* **1988**, *41*, 1915. (b) Ichimura, M.; Ogawa, T.; Takahashi, K.; Kobayashi, E.; Kawamoto, I.; Yasuzawa, T.; Takahashi, I.; Nakano, H. *J. Antibiot.* **1990**, *43*, 1037.

(5) Chidester, C. G.; Krueger, W. C.; Mizsak, S. A.; Duchamp, D. J.; Martin, D. G. *J. Am. Chem. Soc.* **1981**, *103*, 7629.

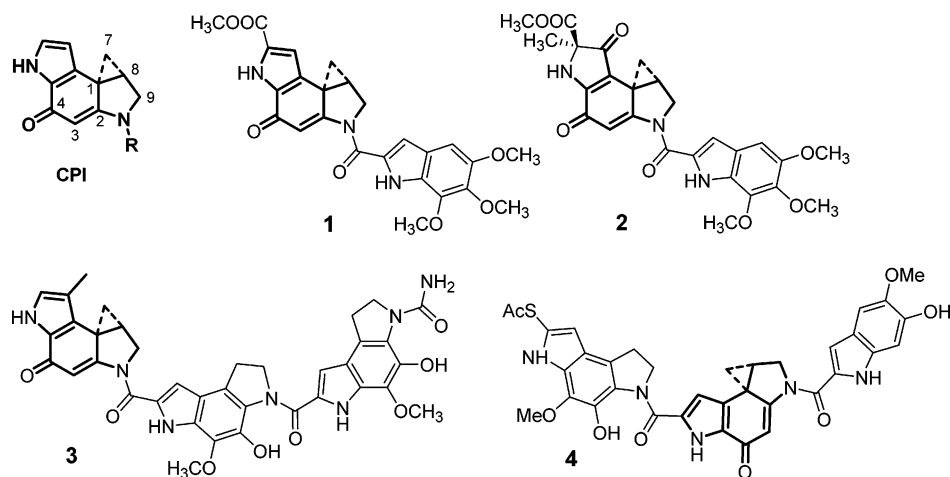
(6) (a) Igarashi, Y.; Futamata, K.; Fujita, T.; Sekine, A.; Senda, H.; Naoki, H.; Furumai, T. *J. Antibiot.* **2003**, *56*, 107. (b) Parrish, J. P.; Kastrinsky, D. B.; Wolkenberg, S. E.; Igarashi, Y.; Boger, D. L. *J. Am. Chem. Soc.* **2003**, *125*, 10971.

(7) Hurley, L. H.; Needham-VanDevanter, D. R. *Acc. Chem. Res.* **1986**, *19*, 230.

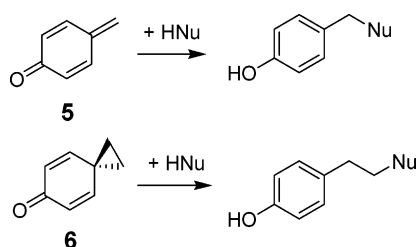
(8) (a) Baird, R.; Winstein, S. *J. Am. Chem. Soc.* **1963**, *85*, 3434. (b) Filar, L. J.; Winstein, S. *Tetrahedron Lett.* **1960**, *25*, 9.

(9) (a) Warpehoski, M. A.; Harper, D. E. *J. Am. Chem. Soc.* **1994**, *116*, 7573. (b) Warpehoski, M. A.; Hurley, L. H. *Chem. Res. Toxicol.* **1988**, *1*, 315.

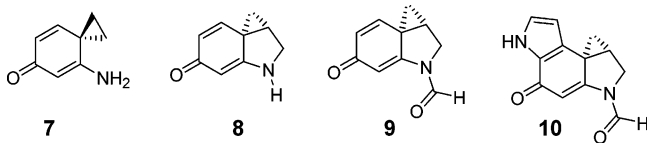
## SCHEME 1



## SCHEME 2



## SCHEME 3



Several structural key features such as the “vinylogous amide conjugation”, that is, conjugation between the nitrogen center and the carbonyl group (which is operative to a different extent in the substrates **7–10**) or the condensed pyrrole ring in **10**, might be expected to significantly contribute to increase stability of the cyclopropylcyclohexadienone moiety, with a concomitant decrease in its reactivity with nucleophiles. CPIs are different from unhindered QMs and other more traditional alkylating agents such as diazonium and phenylnitrenium ions,<sup>13</sup> carbocations,<sup>14</sup> benzyl halides,<sup>15</sup> and quinone methides<sup>10–12,16,17</sup> because they are unreactive toward biological nucleophiles in water solution under neutral

conditions but become highly activated when precomplexed to a DNA duplex, under mild conditions (proceeding in less than 1 h at 4–25 °C).<sup>18</sup> The origin of the selectivity and the source of the catalytic effect in the alkylation reaction with DNA remains quite controversial. In fact, to date two distinct models have emerged from all the investigations focused on this issue. The first one, which was proposed by Hurley and Warpehoski more than a decade ago,<sup>9,19</sup> suggests that the exceptional electrophilicity of CPIs complexed to DNA could be ascribed to an acid catalysis of the environment associated with DNA itself. More recently Boger experimentally tested and proved that Warpehoski’s model of a sequence-dependent backbone phosphate protonation of the C<sub>4</sub>-carbonyl group (Scheme 1 for numbering) is not operative under physiological conditions.<sup>20</sup> In addition, structural data obtained from molecular dynamic studies in a vacuum suggest that the positioning of the proximal backbone phosphates in the adduct of the duocarmycin SA and DNA are much too far from the former C<sub>4</sub> carbonyl center to be engaged in a direct H-bonding.<sup>21,22</sup>

The second model has been more recently proposed by Boger’s group through an extensive and impressive experimental investigation with both simplified<sup>23</sup> and extended analogues of the drug.<sup>24</sup> Several simple synthetic CPI analogues such as those in Scheme 4 have been synthesized and studied,<sup>21</sup> establishing a striking

(10) (a) Chiang, Y. A.; Kresge, J.; Zhu, Y. *J. Am. Chem. Soc.* **2001**, *123*, 8089. (b) Chiang, Y. A.; Kresge, J.; Zhu, Y. *J. Am. Chem. Soc.* **2000**, *122*, 9854. (c) Chiang, Y. A.; Kresge, J.; Zhu, Y. *J. Am. Chem. Soc.* **2002**, *123*, 717. (d) Wan, P.; Barker, B.; Diao, L.; Fisher, M.; Shi, Y.; Yang, C. *Can. J. Chem.* **1996**, *74*, 465. (e) Brousmiche, D.; Wan, P. *Chem. Commun.* **1998**, 491.

(11) (a) Modica, E.; Zanaletti, R.; Freccero, M.; Mella, M. *J. Org. Chem.* **2001**, *66*, 41. (b) Zanaletti, R.; Freccero, M. *Chem. Commun.* **2002**, 1908.

(12) (a) Di Valentin, C.; Freccero, M.; Zanaletti, R.; Sarzi-Amadè, M. *J. Am. Chem. Soc.* **2001**, *123*, 8366. (b) Freccero, M.; Di Valentin, C.; Sarzi-Amadè, M. *J. Am. Chem. Soc.* **2003**, *125*, 3544. (c) Freccero, M.; Gandolfi, R.; Sarzi-Amadè, M. *J. Org. Chem.* **2003**, *68*, 6411.

(13) Parks, J. M.; Ford, G. P.; Cramer, C. J. *J. Org. Chem.* **2001**, *66*, 8997.

(14) Blans, P.; Fishbein, J. C. *Chem. Res. Toxicol.* **2000**, *13*, 431.

(15) (a) Moschel, R. C.; Hudgins, R. W.; Dipple, A. *J. Org. Chem.* **1986**, *51*, 4180. (b) Moon, K.-Y.; Moschel, R. C. *Chem. Res. Toxicol.* **1998**, *11*, 696.

(16) (a) Rokita, S. E.; Yang, J.; Pande, P.; Shearer, J.; Greenberg, W. A. *J. Org. Chem.* **1997**, *62*, 3010. (b) Pande, P.; Shearer, J.; Yang, J.; Greenberg, W. A.; Rokita, S. E. *J. Am. Chem. Soc.* **1999**, *121*, 6773. (c) Veldhuyzen, W. F.; Shallop, A. J.; Jones, R. A.; Rokita, S. E. *J. Am. Chem. Soc.* **2001**, *123*, 11126. (d) Veldhuyzen, Lam, Y.-F.; Rokita, S. E. *Chem. Res. Toxicol.* **2001**, *14*, 1345.

(17) (a) Lewis, M. A.; Graff Yoerg, D.; Bolton, J. L.; Thompson, J. A. *Chem. Res. Toxicol.* **1996**, *9*, 1368. (b) Zhou, Q.; Turnbull, K. D. *J. Org. Chem.* **1999**, *64*, 2847. (c) Zhou, Q.; Turnbull, K. D. *J. Org. Chem.* **2001**, *66*, 7072.

(18) Boger, D. L.; Garbaccio, R. M. *Acc. Chem. Res.* **1999**, *32*, 1043.

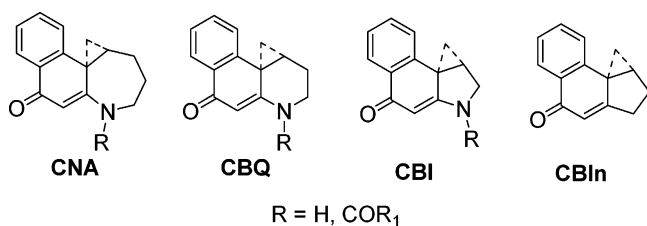
(19) (a) Hurley, L. H.; Reynolds, V. L.; Swenson, D. H.; Petzold, G. L.; Scahill, T. A. *Science* **1984**, *226*, 843. (b) Lin, C. H.; Beale, J. M.; Hurley, L. H. *Biochemistry* **1991**, *30*, 3597. (c) Hurley, L. H.; Warpehoski, M. A.; Lee, C.-S.; McGovren, J. P.; Scahill, T. A.; Kelly, R. C.; Mitchell, M. A.; Wieniensch, N. A.; Gebhard, I.; Johnson, P. D.; Bradford, V. S. *J. Am. Chem. Soc.* **1990**, *112*, 4633.

(20) Yves, A.; Boger, D. L. *Bioorg. Med. Chem. Lett.* **2002**, *12*, 303.

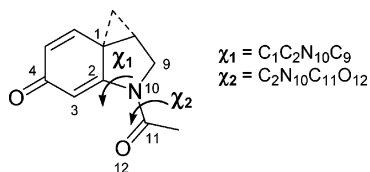
(21) Schnell, J. R.; Ketchum, R. R.; Boger, D. L.; Chazin, W. J. *J. Am. Chem. Soc.* **1999**, *121*, 5645.

(22) (a) Smith, J. A.; Bifulco, G.; Case, D. A.; Boger, D. L.; Gomez-Paloma, L.; Chazin, W. J. *J. Mol. Biol.* **2000**, *300*, 1195. (b) Eis, P. S.; Smith, J. A.; Rydzewski, J. M.; Case, D. A.; Boger, D. L.; Chazin, W. J. *J. Mol. Biol.* **1997**, *272*, 237.

## SCHEME 4



## SCHEME 5



structure–reactivity correlation that can be summarized by the following statements:

(i) The reactivity decrease that occur in the series CNA<sup>23b</sup> > CBQ<sup>23d,e</sup> > CBI<sup>23f</sup> (Scheme 4) are the consequence of the increase of vinylogous amide conjugation.<sup>18</sup>

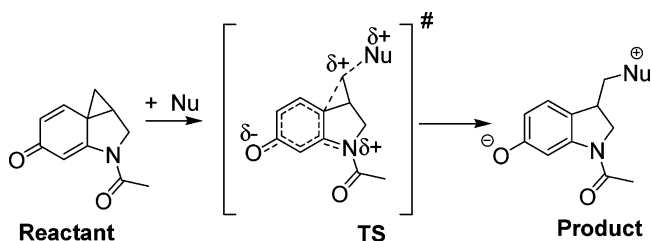
(ii) N-Acylation reduces the vinylogous amide conjugation and increases the reactivity.<sup>24b</sup>

It is quite evident that the vinylogous amide conjugation is strongly affected not only by the homologation of the carbocycle embedding the nitrogen atom N<sub>10</sub> but also by its N-acylation passing from **8** to **9** (Scheme 3). Actually, it may be turned on/of or tuned by conformational changes of the substrate, modifying the values of both dihedral angles C<sub>1</sub>C<sub>2</sub>N<sub>10</sub>C<sub>9</sub> ( $\chi_1$ ) and C<sub>2</sub>N<sub>10</sub>C<sub>11</sub>O<sub>12</sub> ( $\chi_2$ ) as depicted in Scheme 5.

Thus, according to Boger, the dominant activating factor of the DNA catalysis is the disruption of the vinylogous amide conjugation, which is sufficient to provide activation for a nucleophilic addition independent of pH, under physiological conditions. In fact, the author also established through pH rate profiles of a few solvolysis reactions that the requirement for acid catalysis of the DNA alkylation is not necessary, and that the substrates CBQ, CNA, and CBIIn do not require either a specific or a general acid catalysis at pH  $\geq 6$ .<sup>25</sup> Such a unique mode of activation of these alkylating agents has been defined by Boger as “shape-dependent catalysis”.<sup>18</sup> Moreover, Boger has suggested that such a “conformational catalysis” can be directly induced by the DNA binding, which activates the CPI drugs for nucleophilic attack.<sup>21</sup>

To our knowledge the issue of conformational vs acid catalysis of the DNA on CPI reactivity has been addressed so far only with experimental approaches, and only very recently a computational study addressed the issue at the HF level of theory in gas phase.<sup>26</sup> A thorough computational investigation, including solvation effects,

## SCHEME 6



could allow a detailed clarification and a quantitative comparison of the two “triggering” modes, with the goal of improving understanding of such important processes. We decided to start our study by tackling the problem of conformational catalysis in the absence of acid catalysis. Our investigation is aimed at identifying which structural feature and geometric variables are more involved in such an activation in order to provide a firm predictive basis to the use of binding-induced conformational change to trigger a large increase in the reactivity of the CPI drugs. When this part of our work was already completed and this paper was ready for submission we became aware that another group had just independently addressed a few aspects of the mechanism of the acid-catalyzed methanolysis of CPI derivatives.<sup>27</sup> Such a reaction was investigated in the frame of density functional theory with the same basis sets and solvation model used by us to explore the uncatalyzed reactivity of the CPI cyclopropane ring opening by ammonia. Their results, being in full agreement with the available experimental data, confirm the validity of our computational choice and they will be further compared to our findings.

The conformational catalysis proposed by Boger, which is grounded on experimental data and qualitative reasoning, could gain additional strength and consistency from our computational approach. In particular, a theoretical analysis could quantify the role of the vinylogous amide conjugation not only on the energy of the reactants but also on the relative stabilization/destabilization of the TSs. The evaluation of the substituent and conformational effects on the energies of both reactants and TSs is mandatory for properly addressing the role of conformational catalysis. As for the latter aspect, an ab initio hybrid density functional theory method coupled with a polarizable continuum model (PCM) for the depiction of the electrostatic effects of the polar bulk (water as solvent or more likely the DNA double strand) represents a reasonably reliable tool to evaluate the crucial role of the zwitterionic character of the TSs (in Scheme 6) involved in condensed phase reaction of the CPI substrates.

As far as we know there are no theoretical data on the uncatalyzed nucleophilic ring opening of either the cyclopropylcyclohexadienone prototype substrate (**6**) or closer models of the CPI drugs, in solution.

Our strategy in addressing this problem was as follows: first we engineered a computational investigation that could correlate several structural key features of the CPI drugs to their effects on the activation energy of the uncatalyzed nucleophile addition, in the attempt to validate the computational approach by comparison to

(23) (a) Boger, D. L.; Turnbull, P. *J. Org. Chem.* **1998**, *63*, 8004. (b) Boger, D. L.; Turnbull, P. *J. Org. Chem.* **1997**, *62*, 5849. (c) Boger, D. L.; Brunette, S. R.; Garbaccio, R. M. *J. Org. Chem.* **2001**, *66*, 5163. (d) Boger, D. L.; Mesini, P. *J. Am. Chem. Soc.* **1995**, *117*, 11647. (e) Boger, D. L.; Mesini, P. *J. Am. Chem. Soc.* **1994**, *116*, 11335. (f) Boger, D. L.; Munk, S. A. *J. Am. Chem. Soc.* **1992**, *114*, 5487.

(24) (a) Boger, D. L.; Bollinger, B.; Hertzog, D. L.; Johnson, D. S.; Cai, H.; Mesini, P.; Garbaccio, R. M.; Jin, Q.; Kitos, P. A. *J. Am. Chem. Soc.* **1997**, *119*, 4987. (b) Boger, D. L.; Hertzog, D. L.; Bollinger, B.; Johnson, D. S.; Cai, H.; Goldberg, J.; Turnbull, P. *J. Am. Chem. Soc.* **1997**, *119*, 4977.

(25) Boger, D. L.; Garbaccio, R. M. *J. Org. Chem.* **1999**, *64*, 5666.

(26) Nahm, K. *Bull. Korean Chem. Soc.* **2004**, *25*, 69.

(27) Cimino, P.; Improta, R.; Bifulco, G.; Riccio, R.; Gomes-Paloma, L.; Barone, V. *J. Org. Chem.* **2004**, *69*, 2816.

the available experimental data. Second, we explored the effect of conformational changes of reactants and TSs on the CPI reactivity. In particular we focused our search on (i) the role of the nitrogen (N<sub>10</sub>) lone pair involved in the vinylogous amide conjugation with the carbonyl C<sub>4</sub>, and the conformational flexibility of the NH<sub>2</sub> moiety, (ii) the effect of N<sub>10</sub>-formylation, and (iii) the conformational mobility of the formyl group (C<sub>11</sub>, see Scheme 5 for numbering) at the N-atom.

Concerning bulk (solvent) effect we remind that solvent effects on the reactivity have been seldom analyzed in previous experimental studies because of solubility problems of the substrates (in low polar solvent) and also that the dielectric constant assumed for the interior of a nucleic acid double helix<sup>28</sup> is similar to that of acetonitrile. These observations led us to address the above issues not only in gas phase but also in solvent bulk (acetonitrile and water). Particular attention has been paid to water effects on decreasing the alkylation reaction barriers.<sup>29</sup>

## Methods and Computation Details

All calculations were carried out using the A11 version of Gaussian 98<sup>30</sup> program package. All the geometric structures of the reactant and transition states located along the ammonia alkylation pathways by CPI models were fully optimized in gas phase using the hybrid density functional method B3LYP<sup>31</sup> with the 6-31G(d) basis set. It is known that diffuse functions can have an important effect on the energies of anions and in our reactive system a zwitterionic character develops in the TSs, with a partial negative charge on the carbonyl oxygen atom. To assess the best compromise between the best basis set and the computationally demanding real systems we optimized the prototype reactants (**6** and **7**) and their related TSs, namely, **S6** and **S7**, also at the B3LYP/6-31+G(d,p) and B3LYP/6-311+G(d,p) both in gas phase and in water solution. Minima and transition states were further verified by vibrational frequency analysis at the same theoretical level, in gas phase. Although the reaction barriers are underestimated for certain types of reactions, DFT methods are currently the most popular method for macromolecular calculations as a result of the computational accuracy at relatively low computational cost.

The bulk solvent effects on geometries and energies of reactants and TSs were calculated via the self-consistent reaction field (SCRf) method using the conductor version of PCM (C-PCM)<sup>32</sup> as implemented in the A11 version of Gaussian 98. The cavity is composed by interlocking spheres centered on non-hydrogen atoms with radii obtained by the HF param-

etrization of Barone known as united atom topological model (UAHF).<sup>33</sup> Such a model includes the nonelectrostatic terms (cavitation, dispersion, and repulsion energy) in addition to the classical electrostatic contribution. For all PCM-UAHF calculations, the number of initial tesserae per atomic sphere was set to 100.

PES (potential energy surface) scans with geometry optimization at each point (relaxed PES) have been performed using the "Opt" keyword, since rigid PES (single point calculation on frozen gas-phase geometry) is the default Gaussian 98 option. The evaluation of the PES in the surrounding of the TSs for the alkylation reactions of ammonia by **7** has been performed locking the forming C<sub>7</sub>-NH<sub>3</sub> bond length at the distance of the real TSs **S7**, while scanning the variables  $\chi_1$ . The dihedral angles  $\chi_1$  (as defined in Scheme 5) for the reactant **7**, has been stepped 24 times by 5.0°, from 0° to 120°, in gas and in condensed phase (acetonitrile and water) at B3LYP/6-31G(d) level of theory. The results of the scans are plotted in Figure 6.

## Results and Discussion

**1. Structural Effects on CPI Reactivity.** To address the points mentioned in the Introduction and to clarify the influence of structural features such as vinylogous conjugation, N-formylation, and pyrrole ring condensation on the reactivity of CPIs as alkylating agents, we explore the potential energy surfaces (PESs) of the uncatalyzed alkylation reactions of ammonia by spiro-cyclopropylcyclohexadienone (**6**), its 3-amino derivative (**7**), the cyclic analogue 1,1a,2,3-tetrahydro-5H-cycloprop[*c*]indol-5-one (**8**), its N-formyl derivative **9**, and a closer model of the drug **10** (Scheme 3) in gas phase and in solvent bulk. Studying the reactivity of more complex (and therefore more computationally demanding) substrates than the prototype **6** and **7** is mandatory, since the comparison with the Boger's experimental results, which is crucial for the computational model validation, is possible only for the substrates **8**–**10**.

**1.1. Reactivity of Parent Cyclopropylcyclohexadienone and Its 3-Amino Analogue in Gas Phase and in Solvent Bulk. General Mechanism. S<sub>N</sub>1- vs S<sub>N</sub>2-like Cyclopropyl Ring Opening.** Exploring the PESs of the alkylation reactions of ammonia in solvent bulk by the parent cyclopropylcyclohexadienone (**6**) and its 3-amino analogue (**7**), we located two types of TSs, namely, **S6**, **S7** and **S6i**, **S7i** (Figure 1). The former TSs (**S6**, **S7**), where the ammonia adds from the backside of the bond C<sub>1</sub>-C<sub>7</sub> undergoing cleavage (with length 1.95 and 1.97 Å, respectively, in water solution), clearly show S<sub>N</sub>2-like character.

In the TSs **S6i** and **S7i** the nucleophilic attack takes place *syn* to the cleaving bonds. These TSs displays S<sub>N</sub>1-like character as a result of a more pronounced breaking of the C<sub>1</sub>-C<sub>7</sub> bond (length 2.21 and 2.29 Å, respectively, in water) in comparison to that of **S6** and **S7**, while also the C<sub>7</sub>-NH<sub>3</sub> distance is slightly larger. Since **S6** and **S7** are much more stable than the related "in" counterparts by more than 20 kcal mol<sup>-1</sup> in water bulk, we will neglect

(28) Roberts, C.; Bandaru, R.; Switzer, C. *J. Am. Chem. Soc.* **1997**, *119*, 4640.

(29) Although the solvent effects on a reaction that produces zwitterionic species from neutral reactants play as expected a key role, the only computational study that addressed so far the catalyzed vs uncatalyzed reactivity of CPI has been performed in gas phase (ref 26).

(30) Frisch, M. J.; Trucks, G. W.; Schlegel, H. B.; Scuseria, G. E.; Robb, M. A.; Cheeseman, J. R.; Zakrzewski, V. G.; Montgomery, J. A., Jr.; Stratmann, R. E.; Burant, J. C.; Dapprich, S.; Millam, J. M.; Daniels, A. D.; Kudin, K. N.; Strain, M. C.; Farkas, O.; Tomasi, J.; Barone, V.; Cossi, M.; Cammi, R.; Mennucci, B.; Pomelli, C.; Adamo, C.; Clifford, S.; Ochterski, J.; Petersson, G. A.; Ayala, P. Y.; Cui, Q.; Morokuma, K.; Rega, N.; Salvador, P.; Dannenberg, J. J.; Malick, D. K.; Rabuck, A. D.; Raghavachari, K.; Foresman, J. B.; Cioslowski, J.; Ortiz, J. V.; Baboul, A. G.; Stefanov, B. B.; Liu, G.; Liashenko, A.; Piskorz, P.; Komaromi, I.; Gomperts, R.; Martin, R. L.; Fox, D. J.; Keith, T.; Al-Laham, M. A.; Peng, C. Y.; Nanayakkara, A.; Challacombe, M.; Gill, P. M. W.; Johnson, B.; Chen, W.; Wong, M. W.; Andres, J. L.; Gonzalez, C.; Head-Gordon, M.; Replogle, E. S.; Pople, J. A. *Gaussian 98*, Revision A.11.3; Gaussian Inc.: Pittsburgh, PA, 2002.

(31) (a) Becke, A. D. *J. Chem. Phys.* **1993**, *98*, 1372. (b) Schmider, H. L.; Becke, A. D. *J. Chem. Phys.* **1998**, *108*, 9624.

(32) (a) Barone, V.; Cossi, M. *J. Phys. Chem. A* **1998**, *102*, 1995. For the original COSMO model, see: (a) Klamt, A.; Schuurmann, J. *Chem. Soc., Perkin Trans.* **1993**, *2*. (b) Klamt, A.; Jonas, V.; Bürger, T.; Lohrenz, J. C. W. *J. Phys. Chem. A* **1998**, *102*, 5074 (b) For a more comprehensive treatment of solvation models see: (c) Cramer, C. J.; Truhlar, D. G. *Chem Rev.* **1999**, *99*, 2161.

(33) Barone, V.; Cossi, M.; Tomasi, J. *J. Chem. Phys.* **1997**, *107*, 3210.

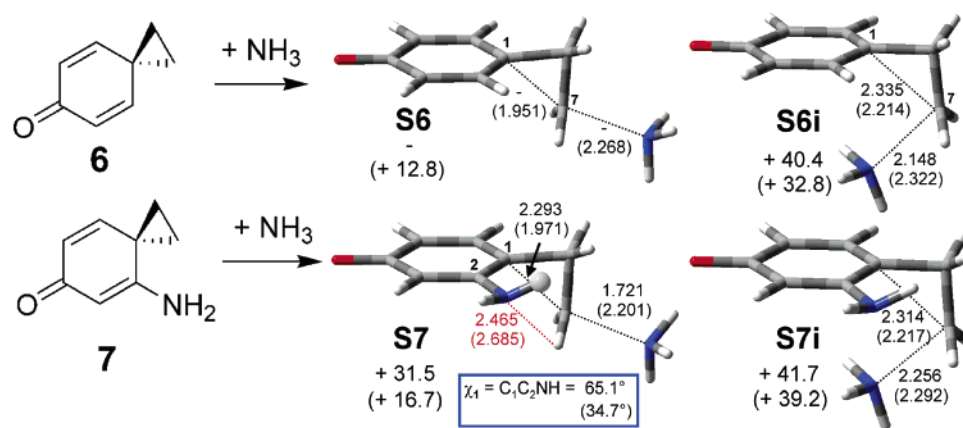


**FIGURE 1.** TSs of ammonia alkylation by **6** and **7** in gas phase and in water. Reaction activation energies (in kcal mol<sup>-1</sup>) and distances (in Å) both in gas phase and in water solution (in parentheses), at the B3LYP/6-31G(d) level.

**TABLE 1.** Activation Energies (kcal mol<sup>-1</sup>)<sup>a</sup> of the TSs Governing the Addition of Ammonia to **6** and **7** at the B3LYP Level with Different Basis Sets

TS	B3LYP/6-311+G(d,p)// B3LYP/6-31G(d)		
	6-31G(d)	6-31+G(d,p)	6-311+G(d,p)
Gas Phase			
<b>S6</b>	30.4 <sup>b</sup>	30.8	31.6
<b>S7</b>	31.5	32.1	32.7
			32.4
Water Solution (C-PCM) <sup>c</sup>			
<b>S6</b>	12.8	13.7	13.7
<b>S7</b>	16.7	17.6	17.6

<sup>a</sup> Relative to the isolated reactants, whose energies (Hartree) in gas phase are -56.5479473 (NH<sub>3</sub>), -384.8353292 (**6**), -440.1925555 (**7**), (B3LYP/6-31G(d)); -56.5669851 (NH<sub>3</sub>), -384.8649799 (**6**), -440.2313297 (**7**), (B3LYP/6-31+G(d,p)); -56.5826356 (NH<sub>3</sub>), -384.9421454 (**6**), -440.322143 (**7**), (B3LYP/6-311+G(d,p)); -56.582388 (NH<sub>3</sub>), (**6**), -440.3219742 (**7**), (single point calculations B3LYP/6-311+G(d,p)//B3LYP/6-31G(d)). In water solution: -56.554640 (NH<sub>3</sub>), -384.847371 (**6**), -440.2147302 (**7**), (B3LYP/6-31G(d)); -56.574510 (NH<sub>3</sub>), -384.880459 (**6**), -440.258537 (**7**), (B3LYP/6-31+G(d,p)); -56.589811 (NH<sub>3</sub>), -384.957459 (**6**), -440.349026 (**7**), (B3LYP/6-311+G(d,p)); -56.589521 (NH<sub>3</sub>), -384.957314 (**6**), -440.348630 (**7**), (single point calculations B3LYP/6-311+G(d,p)//B3LYP/6-31G(d)). <sup>b</sup> With the C<sub>7</sub>-NH<sub>3</sub> forming bond distance locked at 1.72 Å. <sup>c</sup> With the inclusion of nonelectrostatic terms.

the S<sub>N</sub>1-like addition and throughout we will consider only S<sub>N</sub>2-like processes.

**1.2. Choice of Basis Set.** Activation energies for the addition of ammonia to **6** and **7** and the most relevant geometrical parameters for **S6** and **S7** TSs, located at B3LYP/6-31G(d), B3LYP/6-31+G(d,p), and B3LYP/6-311+G(d,p) in gas phase and in water solution are listed in Tables 1 and 2. From a geometrical point of view the enlargement of the basis set from 6-31G(d) to 6-311+G(d,p) slightly changes **S7** TS forming bond lengths, less than 0.07 Å, both in gas phase and in water solution. Moreover, the inclusion of the polarization functions in the basis set [6-31+G(d,p) and 6-311+G(d,p)] allowed the localization of **S6** TS and gave the opportunity to compare the reactivity of the two reactive systems in gas phase.

Energies, as expected, are more basis set dependent than geometries, but luckily TSs activation energies do not change considerably on passing from 6-31G(d) to 6-311+G(d,p) basis sets. They are higher only by ~1 kcal mol<sup>-1</sup> with the largest basis sets used, both in gas phase and in water solution.

**TABLE 2.** Representative Geometrical Parameters [Bond Lengths (Å)] in Gas Phase and in Water (in Parentheses) for TSs Governing the Addition of Ammonia to **6** and **7** at the B3LYP Level with Different Basis Sets

TS	6-31G(d)	6-31+G(d,p)	6-311+G(d,p)
C <sub>7</sub> -NH <sub>3</sub> Forming Bond			
<b>S6</b>	— (2.268)	1.752 (2.300)	1.750 (2.299)
<b>S7</b>	1.721 (2.201)	1.786 (2.228)	1.784 (2.228)
C <sub>1</sub> -C <sub>7</sub> Breaking Bond			
<b>S6</b>	— (1.950)	2.300 (1.951)	2.301 (1.959)
<b>S7</b>	2.293 (1.971)	2.251 (1.970)	2.254 (1.977)
N <sub>10</sub> -HC <sub>7</sub> Distance			
<b>S7</b>	2.462 (2.675)	2.542 (2.733)	2.545 (2.738)

These data suggest that the choice of the smaller basis set [6-31G(d)] is an acceptable compromise between computational accuracy and time-consuming calculations, that is, it can be confidently used for relatively large substrates with a closer structure to the CPI drugs, such as **10**.

**1.3. Relative Reactivity of Cyclopropylcyclohexadienone vs Its 3-Amino Analogue: Role of Vinylogous Conjugation.** On passing from **6** to **7** the introduction of vinylogous amide conjugation, according to Boger,<sup>1a,18</sup> should induce a stabilization on the cyclopropylcyclohexadienone structure and therefore should reduce its reactivity as electrophile, if a comparable stabilizing effect is not operative to the same extent in the TS.

In accord to this statement, our computational data (Table 1) with diffuse functions suggest that the spirocyclopropylcyclohexadienone (**6**) is slightly more reactive than its 3-amino analogue (**7**) in gas phase by 1.1–1.3 kcal mol<sup>-1</sup> and such an energy gap is substantially not basis set dependent (Table 1). The reactivity gap becomes larger in water solution where **7** displays a higher activation energy in comparison to that of **6**, by at least 3.9 kcal mol<sup>-1</sup>, in full agreement with Boger's original hypothesis. The enlargement of the reactivity gap caused by the solvent is partially due (~1 kcal mol<sup>-1</sup>) to the higher relative electrostatic stabilization of the reactants (**7** vs **6**, which is -11.0 kcal mol<sup>-1</sup>) in comparison to that of the TSs (**S7** vs **S6**, which is -10.1 kcal mol<sup>-1</sup>).

As expected for a reaction that produces a zwitterion from neutral reactant, TS geometries are obviously very

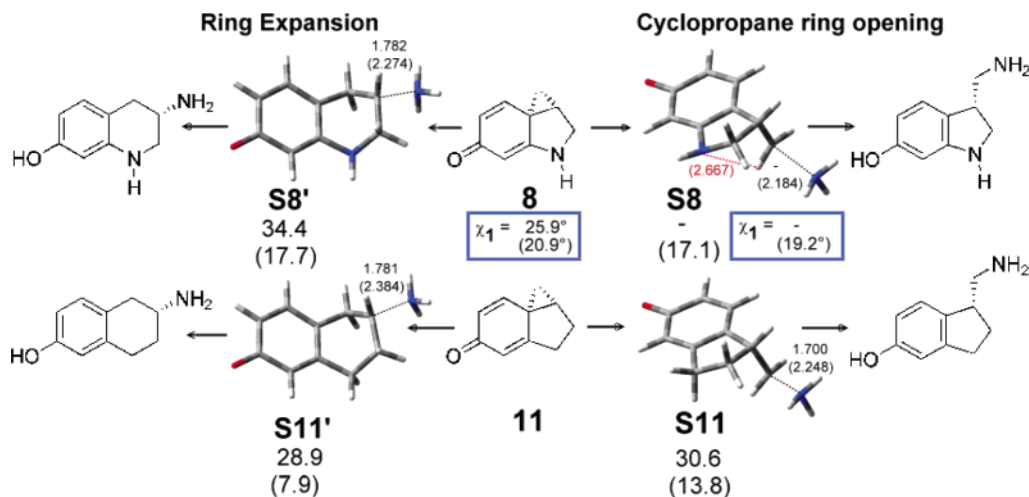


**FIGURE 2.** TSs of ammonia alkylation by **8** and **11** in gas phase and in water (in parentheses). On the right side is reported the cyclopropane ring opening, and on the left side is depicted the ring expansion process. Activation energies (in kcal mol<sup>-1</sup>) and bond lengths (in Å) are reported at the B3LYP/6-31G(d) level.

“late” in gas phase. The forming C–NH<sub>3</sub> bond can be considered as a stretched CH<sub>2</sub>–NH<sub>3</sub><sup>+</sup> group, with an important charge transfer from ammonia to the electrophile [+0.39e and +0.36e CHelpG charges at B3LYP/6-311+G(d,p) level of theory]. The presence of an induced positive charge on CH<sub>2</sub> and the fact that the nitrogen atom of the NH<sub>2</sub> moiety in **S7** is at fairly close distance [at 2.46 Å using 6-31G(d) and at 2.54 Å with 6-311G+(d,p) basis set] should lead to an intramolecular CH–N(10) hydrogen-bonding (the red dotted lines in Figure 1), similar to that between cationic species such as quaternary cations (i.e., tetramethylammonium) and N-donors such as MeNH<sub>2</sub> and Me<sub>3</sub>N ( $\Delta H^{\ddagger} \sim 8$  kcal mol<sup>-1</sup>).<sup>34</sup> Consistent with this hypothesis the sum of N and H van der Waals radii (2.7 Å) is higher than the CH–N<sub>10</sub> distance. Similar geometrical features have been used by Houk<sup>35</sup> and us<sup>36</sup> to rationalize the syn attack of peracids to the homoallylic CH<sub>2</sub>X group as a result of CH–O hydrogen-bonding. The strength of the CH–O hydrogen-bonding in the epoxidation reaction was enhanced by electronegative substituent on the homoallylic CH<sub>2</sub>.

The optimized TSs in water bulk obviously differ greatly from the gas-phase structures, and their character is “early”, with a C–N forming bond (2.20–2.23 Å) much more elongated than that in gas phase. The change induced by the solvent should lessen the importance of the intramolecular H-bonding in **S7** as shown by a slight increase in the CH–N<sub>10</sub> distance in water solution (see data in Table 2).

The quantitative evaluation of the effects controlling such a reactivity gap and in particular the role of the vinylogous stabilization on the reactants (**7** vs **6**) and TSs (i.e., **S7** vs **S6**) will be extensively addressed in the section Conformational Effects on CPI Reactivity.

#### 1.4. Effect of a Nitrogen Atom Embedded in a Pyrrolidine Ring on Reactivity and Selectivity. The

(34) Meot-Ner, M.; Deakyne, C. A. *J. Am. Chem. Soc.* **1985**, *107*, 469.

(35) Washington, I.; Houk, K. N. *Angew. Chem., Int. Ed.* **2001**, *40*, 4485

(36) Freccero, M.; Gandolfi, R.; Sarzi-Amadè, M. *Tetrahedron* **1999**, *55*, 11309.

**TABLE 3.** Relative Energies (kcal mol<sup>-1</sup>)<sup>a</sup> of TSs Governing the Addition of Ammonia to **8** and **11** at the B3LYP Level with Different Basis Sets

TS	6-31G(d)	6-31+G(d,p)
Gas Phase		
<b>S8</b>	<i>b</i>	34.6
<b>S8'</b>	34.4	35.0
<b>S11</b>	30.6	31.2
<b>S11'</b>	28.9	29.8
Water Solution (C-PCM) <sup>c</sup>		
<b>S8</b>	17.1	18.2
<b>S8'</b>	17.7	18.4
<b>S11</b>	13.8	14.5
<b>S11'</b>	7.9	13.7

<sup>a</sup> Relative to the isolated reactants, whose energies (Hartree) in gas phase are –56.5479473 (NH<sub>3</sub>), –478.2972539 (**8**), –462.2599355 (**11**), [B3LYP/6-31G(d)]; –56.5669851 (NH<sub>3</sub>), –478.332968 (**8**), –462.2927887 (**11**), [B3LYP/6-31+G(d,p)]. In water solution: –56.554640 (NH<sub>3</sub>), –478.320427 (**8**), –462.273229 (**11**), [B3LYP/6-31G(d)]; –56.574510 (NH<sub>3</sub>), –384.880459 (**8**), –440.258537 (**11**), [B3LYP/6-31+G(d,p)]. <sup>b</sup> Unable to locate **S8**. <sup>c</sup> With the inclusion of nonelectrostatic terms.

further step in analyzing model compounds to unravel factors that control the reactivity of CPIs is to address reactivity and chemoselectivity of the reacting core of those drugs, i.e., 1,1a,2,3-tetrahydro-5*H*-cycloprop[*c*] indol-5-one (**8**). Herein, we report the alkylation of ammonia by **8** without acid catalysis and its comparison with the carbocyclic analogue **11** (Figure 2).

First, we located TS **S8** (Figure 2), which displays a higher activation energy ( $\Delta E^{\ddagger} = 34.6$  kcal mol<sup>-1</sup>, Table 3) than that of **S7** ( $\Delta E^{\ddagger} = 32.1$  kcal mol<sup>-1</sup>, Table 1) in gas phase at B3LYP/6-31+G(d) level. Such a difference (+2.5 kcal mol<sup>-1</sup>), which becomes smaller in water solution (+0.6 kcal mol<sup>-1</sup>), could be the result of the conformational constraint induced by the carbocycle in the TS. In fact **S7**, unlike **S8**, is conformationally flexible and is capable of adjusting the angle  $\chi_1$  in order to maximize stabilizing effects. However, the reactants (**8** vs **7**) display very similar  $\chi_1$  angles (21.4° and 20.9° for **7** and **8** in water, respectively) and consequently should benefit by an almost identical vinylogous amide stabilization. Therefore the lowering of the reactivity induced by

the constraint of a pyrrolidine ring in comparison to a conformational free  $\text{NH}_2$  group is not due to a different extent of the vinylogous amide stabilization of the reactants but has to be mainly ascribed to TS effects, namely, selective stabilization of **S7** vs **S8**. In fact,  $\chi_1$  in **S7** [62.3° and 31.3°, in gas and in water, respectively, with 6-31+G(d,p) basis sets] is quite different from that in **S8** (20.6° and 19.2°, in gas and in water, respectively), both in gas phase and in water solution. This angle adjustment turns the nitrogen lone pair toward the cyclopropane methylene hydrogen and (i) slightly favors  $\text{CH}-\text{N}_{10}$  hydrogen-bonding and, more importantly, (ii) gives rise to a decrease in conjugation with the carbonyl group. It should be noted that a decrease of such a conjugation in TS **S7** vs **S8**, as shown by the higher negative charge on the  $\text{N}_{10}$  atom (CHelpG charges  $-0.870\text{e}$  in **S7** vs  $-0.734\text{e}$  in **S8**, in gas phase), should increase the electron-accepting capacity of the cyclohexanone ring, favoring the development of a negative charge on the  $\text{C}_1$  in **S7** (CHelpG  $-0.245\text{e}$ ) in comparison to that of the related carbon atom in **S8** ( $-0.123\text{e}$ ).

The cyclopropane ring opening for substrate **8**, promoted by ammonia attack, displays a higher activation energy in comparison to that of the carbocyclic analogue **11** both in gas phase (by  $+3.4 \text{ kcal mol}^{-1}$ ) and in water (by  $+3.7 \text{ kcal mol}^{-1}$ ), as shown by the data in Table 3.

The predicted reactivity gap between **8** and **11** parallels the experimental one between the benzo analogues CBI and CBI $\text{n}$  (Scheme 4), which is quantified in the solvolytic rate constants measured by Boger under acid catalysis at pH 3.<sup>23a</sup> This computational evidence confirms that the loss of vinylogous stabilization in the reactant passing from **8** to **11** is partially responsible for the observed increase in reactivity.

Our computational model goes beyond the ability of predicting the relative reactivity of **8** and **11** in water. In fact, it also reproduces the switch in selectivity from near exclusive ring expansion addition of ammonia to predominant ring opening passing from substrate **11** to **8** (see activation energy data in Figure 2).

Boger rationalized the difference in chemoselectivity of the alkylation process for several CPI-like alkylating agents as mainly due to intrinsic stereoelectronic effect of the substrate (i.e., alignment of the cyclopropane  $\sigma$  bond, undergoing ammonia addition, to the  $\pi$  system), which was evaluated (when available) by X-ray structure. Unfortunately X-ray structure for CBI $\text{n}$  was not provided, and the experimentalists could not test the generality of such a hypothesis on CBI and CBI $\text{n}$  structures. On the other hand, no difference in stereoelectronic effect is expected between **8** and **11** since their computed geometries are almost superimposable. Thus the inversion of the chemoselectivity passing from the substrate **11** to the nitrogen analogue **8** must be ascribed to other factors. We believe that the steric H–H interaction in **S11** between the methylene undergoing attack and the distal methylene in the five-membered ring, which are at only 2.45 Å, in water [at B3LYP/6-31G(d)] can be held responsible of its higher energy relative to **S11'**. As far as competition between **S8** and **S8'** one can notice that weak stabilizing H-bonding interaction involving the cyclic nitrogen atom and the  $\text{CH}_2$  undergoing addition (where the distance between the hydrogen donor acceptor centers is 2.63 Å in gas phase and 2.68 Å in water at

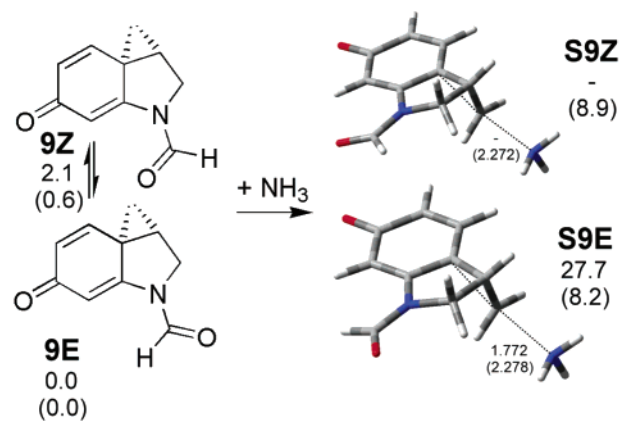


**FIGURE 3.** TSs of ammonia alkylation by **9** in gas phase and in water (in parentheses). Reaction activation energies (in  $\text{kcal mol}^{-1}$ ) and bond lengths (in Å) at the B3LYP/6-31G(d) are reported.

**TABLE 4.** Energies ( $\text{kcal mol}^{-1}$ )<sup>a</sup> of Reactant Conformers and Activation Energy for Ammonia Addition to **9Z** and **9E** at the B3LYP Level with Different Basis Sets, in Gas Phase and in Water

structure	gas		water	
	6-31G(d)	6-31+G(d,p)	6-31G(d)	6-31+G(d,p)
<b>9Z</b>	2.1	2.4	0.6	0.8
<b>S9Z</b>		35.0	8.9	15.0
<b>S9E</b>	27.7	28.6	8.2	13.9

<sup>a</sup> Relative to the most stable **9E** isomer. <sup>b</sup> Relative to the most stable **9E** isomer and ammonia.

B3LYP/6-31+G(d,p)) is operative in the TS **S8** but not in **S8'**, where the nitrogen lone pair displays a *trans* geometry relative to the hydrogen atom on the carbon undergoing addition. Moreover, inductive effects (through the  $\sigma$ -bond frame) destabilize TS **S8'** relative to **S8**. In fact, in the latter TS, one more  $\sigma$ -bond separates the carbon undergoing ammonia addition (which displays carbocationic character) to the electron-withdrawing cyclic nitrogen  $\text{N}_{10}$ , also compensating the fact that the positively charged carbon center is secondary in **S8'** and primary in **S8**.

**1.5. Effect of N-Formylation.** According to Boger's experimental data,<sup>18,22b</sup> N-acylation increases the solvolysis reactivity of CPI substrates. To reproduce the reactivity enhancement induced by N-acylation and to validate our computational model by comparison to the experimental data, we first studied the reactivity of **9** toward ammonia and then compared it to that of **8**.

Substrate **9** exists as a mixture of two equilibrating conformers, **9E** and **9Z**. The *E* isomer is more stable than the *Z* one in gas phase by more than  $2 \text{ kcal mol}^{-1}$ , but in water solution their energy is comparable (Table 4). We were able to locate two TSs along the reaction coordinate in gas phase with diffuse functions (**S9E** and **S9Z**), arising from the ammonia addition to the **9E** and **9Z**, respectively.

We managed also to locate them in water bulk, where they are much more stable than in gas phase. The zwitterionic nature of TSs is responsible of the massive

stabilization brought about by water bulk effects on both TSs **S9**, in comparison to gas phase, which is similar to that calculated for TSs **S6** and **S7**.

The lowering of the activation energy for the ammonia alkylation reaction by **9** in comparison to that by **8** (see data in Tables 3 and 4) in both gas phase and in water solution is the quantitative computational evaluation of the *N*-formyl substitution effect, which significantly enhances the reactivity of the substrate by 6.0 and 4.3 kcal mol<sup>-1</sup> (**S9E** vs **S8**) in gas phase and in water, respectively, at B3LYP/6-31+(d,p) level. A similar enhancement of the reactivity induced by *N*-*tert*-butoxycarbonyl substitution, with the reduction of the activation energy by -5.9 kcal mol<sup>-1</sup>, has been reported by Barone for the acid-catalyzed methanolysis in methanol as solvent.<sup>27</sup>

*N*-Formylation effect on CPI reactivity could be the result of synergic effects operating on the destabilization of the reactant (**9E** vs **8**) and on the stabilization of TS (**S9E** vs **S8**). The decreased stabilization of the reactant **9E** (in comparison to **8**), could be the result of the reduction of the vinylogous amide conjugation as a result of the competition of the formyl moiety for the N<sub>10</sub> nitrogen lone pair. The increase TS stabilization of **S9E** (vs **S8**) may be ascribed to (i) the reduced electron-donating conjugation of N<sub>10</sub> atom and (ii) the increased inductive electron-attracting ability of *N*<sub>10</sub>-formyl in delocalizing the developing negative charge on the cyclohexadienone moiety. The quantitative comparison of these two effects will be addressed in Conformational Effects on CPI Reactivity.

**1.6. Effect of Pyrrole Ring Condensation.** The effect of pyrrole ring condensation to the quinonoid ring of CPI drugs on the reactivity as alkylating agent has been investigated and compared to benzo analogue CBI by Boger, only under acid catalysis (at pH 3).<sup>37</sup> To our knowledge no comparative data between substrates with and without such a structural feature have so far been reported in the literature, under neutral condition (i.e., without acid catalysis). The reason for the missing experimental data is the exceptional stability under solvolytic condition at pH 7 of a substrate like **10**. To assess the role of the condensed pyrrole ring on the reactivity of CPI structures without acid catalysis, we investigated the reactivity of a closer model of the drugs, locating both minimum and TS of the ammonia alkylation by **10** in gas phase and in water at B3LYP/6-31G(d) level of theory (Figure 4).

Similarly to **9** the substrate **10** exists as a mixture of two equilibrating conformers **10E** and **10Z**. Once again, the *E* isomer is more stable than the *Z* form both in gas phase (by -2.0) and in water (-0.8 kcal mol<sup>-1</sup>). We were able to locate the TS **S10** for the ammonia alkylation by the *E* isomer both in gas phase and water solution. The effect of the pyrrole ring on reactivity, in gas phase, can be evaluated by activation energy comparison between **S10E** and **S9E** ( $\Delta E^\ddagger = 31.5$  and 27.7 kcal mol<sup>-1</sup>, in gas phase, respectively). The activation energy enhancement induced by the pyrrole-conjugated ring is already significant in gas phase (+4.0 kcal mol<sup>-1</sup>) but becomes remarkably much higher in water solution (+8.9 kcal

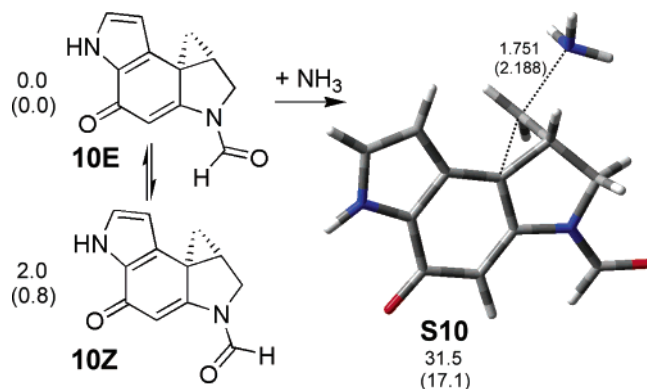


**FIGURE 4.** TS of ammonia alkylation by **10** in gas phase and in water (in parentheses). Reaction activation energies (in kcal mol<sup>-1</sup>) and bond lengths (in Å) are reported with 6-31G(d) basis sets.

mol<sup>-1</sup>). The very same structural modification (i.e., pyrrole ring condensation) on *N*-*tert*-butoxycarbonyl derivatives, investigated by Barone, gives rise to a comparable enhancement of the activation energy (by +5.9 kcal mol<sup>-1</sup>) for the acid-catalyzed methanolysis.<sup>27</sup>

The comparison of our computational **9/10** rate ratio ( $3.3 \times 10^6$  in water bulk) to the experimental solvolysis relative rates determined spectrophotometrically at pH 3 by Boger (experimental reactivity rate ratio **9/10** =  $3.7 \times 10^3$ ) reveals that the reactivity gap between **9** and **10** is strongly enhanced passing from an acid catalyzed to an uncatalyzed addition process.

The structural effects of the pyrrole ring and the *N*-formyl substitution on the reactivity of the spirocyclopropylcyclohexadienones are opposite and of comparable magnitude, since the activation energy in water solution for both **8** and **10** is the very same, i.e., 17.1 kcal mol<sup>-1</sup>, at B3LYP/6-31G(d).

## 2. Conformational Effects on CPI Reactivity.

**2.1. Conformational Effects on Activation of 3-Aminospirocyclopropylcyclohexadienone.** We have shown that the amino derivative **7** is less reactive than the unsubstituted analogue **6** and that such a difference in reactivity is much more pronounced in water solution than in gas phase. To clarify if such a reactivity gap is the results of (i) ground-state effects (i.e., vinylogous amide stabilization of the reactant **7** vs **6**)<sup>38</sup> and/or (ii) TS differential stabilization (**S6** vs **S7**), we first performed the conformational analysis of reactant **7**, locating the conformational TSs **TS-0°**, **TS-120°**, and **TS-300°** (Figure 5) for a quantitative evaluation of the NH<sub>2</sub> inversion and its rotational barrier around the N<sub>10</sub>-C<sub>2</sub> bond, both in gas phase and in water solution.

The global fully optimized minimum of substrate **7** in gas phase corresponds to a structure with  $\chi_1 = 37.7^\circ$ , with the NH<sub>2</sub> group slightly pyramidalized and with a small or negligible barrier in gas phase and in water, respectively (<1 kcal mol<sup>-1</sup>, see Table 5) for the inversion via the planar **TS-0°**. The effect of the cross-conjugated vinylogous amine on the stability of the reactant can be computationally evaluated locating the **TS-120°** where the nitrogen lone pair of the now strongly pyramidalized NH<sub>2</sub> is coplanar to the quinone ring for  $\chi_1 = 120^\circ$  (syn to the cyclopropane ring). Since in the conformational **TS-120°** the nitrogen lone pair is orthogonal to the

(37) Boger, D. L.; Mésini, P.; Tarby, C. M. *J. Am. Chem. Soc.* **1994**, *116*, 6461.



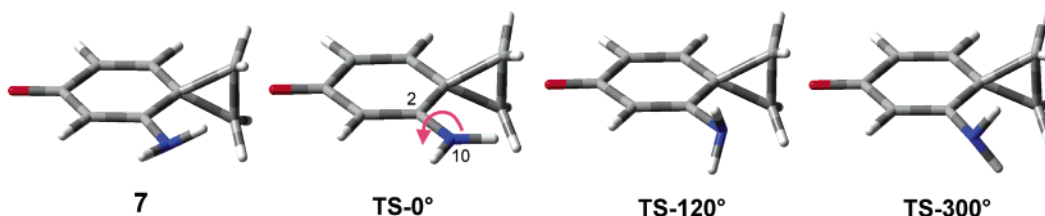


FIGURE 5. Conformational TSs for the inversion and rotation of the NH<sub>2</sub> group in 7.

TABLE 5. Relative Energies (kcal mol<sup>-1</sup>)<sup>a</sup> of TSs Governing Inversion and Rotation of the NH<sub>2</sub> Group around the C<sub>2</sub>-N<sub>10</sub> Bond in Reactant 7 at the B3LYP Level with Different Basis Sets, in Gas Phase and in Water Solution (in Parentheses)

structure	6-31G(d)	6-31+G(d,p)
TS-0°	0.85 (0.08)	0.48 ( <i>b</i> )
TS-120°	6.04 (9.68)	6.14 (10.69)
TS-300°	8.63 (10.29)	8.71 (11.02)

<sup>a</sup> Relative to the reactant minimum 7. <sup>b</sup> We were unable to locate TS-0° in water bulk with 6-31+G(d,p) basis sets, since it collapsed to 7.

quinone  $\pi$ -system (i.e., coplanar to the cyclohexadienone ring) and cannot be delocalized on the carbonyl oxygen atom, its energy relative to the real conformational minimum 7 gives a quantitative evaluation of the reactant destabilization induced mostly by complete loss of vinylogous conjugation (see data in Table 5). Such a rotational barrier is almost unaffected by the addition of the polarized functions in gas phase, where it reaches 6.1 kcal mol<sup>-1</sup>, a value very similar to that computed at MP2/6-311G(d,p)//HF/6-31G(d) by Head-Gordon and Pople<sup>39</sup> for vinylamine (5.7 kcal mol<sup>-1</sup>) and slightly higher than the rotational barrier computed by the same authors for aniline (4.3 kcal mol<sup>-1</sup>).

The rotational barrier significantly rises passing from gas phase to water solution where, although higher than 10 kcal mol<sup>-1</sup> (see data in Table 5), it still remains lower than the rotational barrier of formamide (15.7 kcal mol<sup>-1</sup> computed at HF/6-31G(d);<sup>40</sup> 18.9 kcal mol<sup>-1</sup> experimental)<sup>41</sup>.

The rising of the rotational barriers passing from gas phase to water solution (Table 5) suggest that *the solvent enhances the vinylogous amide conjugation in the reactant 7 through its electrostatic effect*, by favoring the related charge separation that is definitely larger in the conformational minimum 7 ( $\mu = 10.4$  D) than in TS-120° ( $\mu = 6.8$  D).<sup>43</sup> The TS-300° resides at a slightly higher energy than TS-120° (see the rotational barrier in Table 5) as a result of the opposite NH<sub>2</sub> pyramidalization that gives rise to repulsive steric interaction between the NH<sub>2</sub> and the cyclopropane ring hydrogens in the former TS (2.22 Å, gas-phase H-H distance).

In addition we have optimized the reactant 7 in gas and condensed phases (acetonitrile and water) while

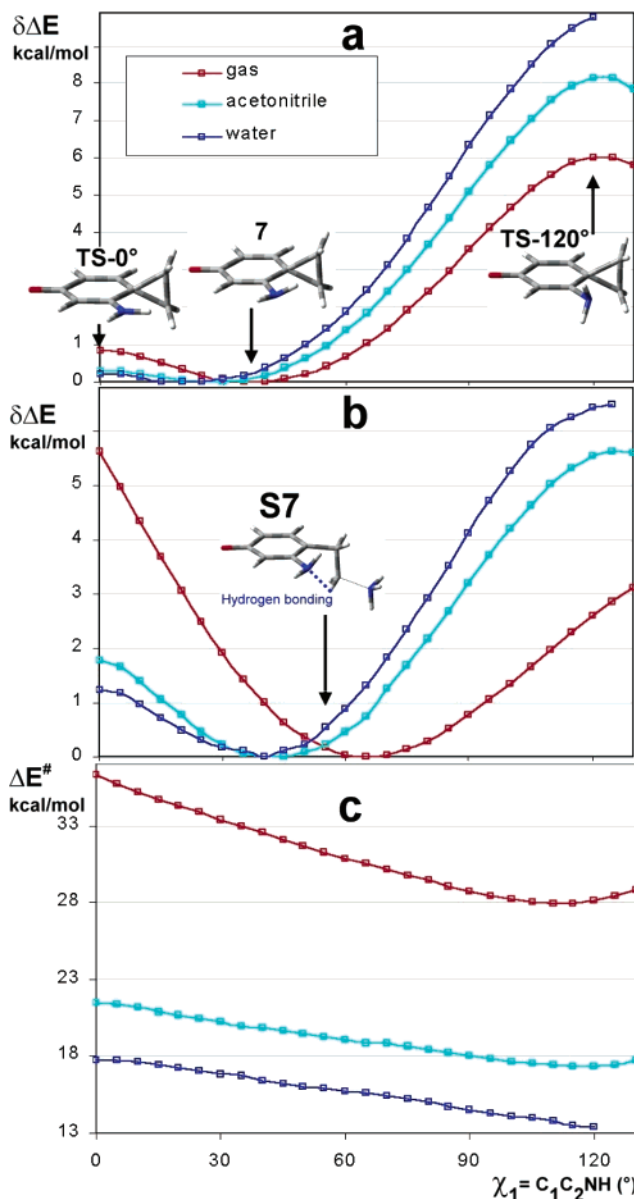


FIGURE 6. Condensed phase vs gas phase conformational effect on the energies of (a) the reactant 7 and (b) the S7 TS and (c) on the reaction activation energy passing from gas phase (red line), acetonitrile (light blue line), and in water (dark blue line), at the B3LYP/6-31G(d) level.

gradually changing the angle  $\chi_1$  by 5° steps in order to evaluate the progressive conformational effect of the NH<sub>2</sub> rotation on the reactant potential energy. The resulting potential energy profile in gas phase, acetonitrile, and in water are reported in Figure 6a.

We have applied a similar approach to evaluate the conformational effect of the dihedral angle  $\chi_1$  on the

(38) DFT and MP2 calculation have been already used to investigate only the degree of reactant destabilization for *N*-acetyl-duocarmycins SA, by locking  $\chi_1$  and  $\chi_2$  angles in gas phase. Kirschner, K. N.; Lee M.; Stanley, R. C.; Bowen, J. P. *Bioorg. Med. Chem.* **2000**, *8*, 329.

(39) Head-Gordon, M.; Pople, J. A. *J. Phys. Chem.* **1993**, *97*, 1147.

(40) Knight, E. T.; Allen, L. C. *J. Am. Chem. Soc.* **1995**, *117*, 4401.

(41) Kamei, H. *Bull. Chem. Soc. Jpn.* **1968**, *41*, 2269.

(42) Dipole moments calculated with 6-31G(d) basis sets in water bulk.

(43) Walsh, A. D. *Trans. Faraday Soc.* **1949**, *45*, 179.

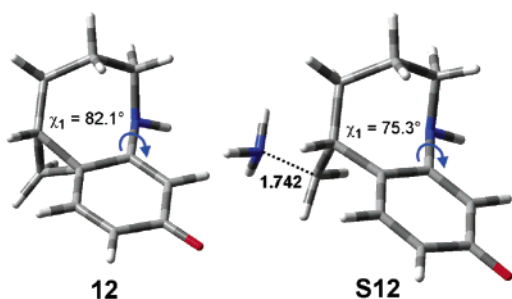


**FIGURE 7.** Substrate **12** and one of the most stable TS for the ammonia alkylation reaction in gas phase (**S12**), at the B3LYP/6-31G(d) level of theory.  $\chi_1$  angle values are reported.

potential energy of TS, locking the C<sub>7</sub>–NH<sub>3</sub> forming bond to the values of the real TS **S7** in gas phase (at 1.72 Å) and in water (at 2.20 Å), while scanning the geometric variable  $\chi_1$ . The resulting energy profiles are reported in Figure 6b. Although it is important to keep in mind that such an approach is approximate since the geometries of the points on the potential energy surface are not real TSs, several quantitative mechanistic consideration can be inferred by the comparison of the two energy profiles in Figure 6a and b.

The difference between the energy profiles of the reactant and TS as a function of  $\chi_1$  is striking, since the TS energy drops much more rapidly than the reactant energy passing from 0° to 60° and rises with a slope lower than that of reactant from 60° to 120°. To use data of Figure 6a and b for a mechanistic analysis we assume that the  $\chi_1$  angle remains constant on passing from reactant to TS, as is the case for the reaction of compounds **8**–**11** where the nitrogen atom is embedded in a ring. This assumption allowed us to evaluate the trend in the reaction activation energy as a function of  $\chi_1$  (Figure 6c) and to what extent it depends on stabilization/destabilization of either reactant or TS.

The resulting reaction activation energy, computed with the above approximate procedure, steeply and linearly drops from 36.3 to 27.9 kcal mol<sup>-1</sup> by the torsion of NH<sub>2</sub> moiety from  $\chi_1 = 0^\circ$  to  $\chi_1 = 110^\circ$ , where the activation energy for the alkylation process in gas phase reaches a minimum (see Figure 6c). It is clear that *such a drop of the activation energy, which can be described as conformational catalysis*, is the result of two distinct and synergic effects, which are tunable by the  $\chi_1$  angle. The first effect, which is operative from 0° to 60° in gas phase and from 0° to 35° in water (Figure 6b) can be ascribed almost entirely to the TS stabilization, since in such a range of  $\chi_1$  values the energy of the substrate is almost constant (within 1 kcal mol<sup>-1</sup>, Figure 6a).

The origin of such a stabilization of the TS could be ascribed to the fact that the rotation of the NH<sub>2</sub> group around the C<sub>2</sub>–N<sub>10</sub> bond lessens the unfavorable steric repulsion between N–H(inner) and the cyclopropane ring, also reinforcing the intramolecular H-bonding between the nitrogen atom of the NH<sub>2</sub> substituent and the CH<sub>2</sub> group undergoing ammonia attack. Such a combination reaches its maximum stabilizing effect of the TS in gas phase (–5.6 kcal mol<sup>-1</sup>) when the nitrogen lone pair points toward the CH<sub>2</sub> hydrogen atom (Figure 7b). In water solution such a stabilizing effect is still operative but is much weaker, according to the fact that in general

H-bonding interactions<sup>12</sup> and in particular the N<sub>10</sub>–HC<sub>7</sub> one (as pointed in section 1.2 by its lengthening in water bulk) become weaker. The second effect is due mainly to the stronger destabilization of the reactant as a function of  $\chi_1$  angle from 60° to 120°, in comparison to the parallel destabilization of the TS, as shown by a steeper rising of the energy profile of the reactant (Figure 7a) in comparison to that of the TS (Figure 7b). Such a destabilization of the reactant, which reaches its maximum at 120° can be ascribed to the complete loss of the vinylogous amide stabilization in the reactants and to destabilization due to closed shell repulsion between the nitrogen lone pair and the cyclopropane ring.<sup>43</sup>

Such an energy trend being operative to a different extent also in water and acetonitrile solution demonstrates that *the conformational catalysis is at work also in a polar bulk* and can affect the reactivity of synthetic drugs where the NH moiety is conformationally more flexible than CPI such as in CBQ and CNA. In fact in CBQ and CNA, where the NH group is embedded in a six- or seven-membered ring, respectively, the  $\chi_1$  angle value may easily reach 100–110°. Actually, we have been able to locate a conformer of the substrate **12** (Figure 7), which is structurally very similar to CNA (for R = H, in Scheme 4) and one of the most stable TSs for the addition of ammonia (**S12**), where the  $\chi_1$  angle is 82.1° and 75.3°, respectively. This evidence suggests that the evaluation of the effect of the  $\chi_1$  angle on the reaction activation energy, even for  $\chi_1 > 75^\circ$  it is worth and meaningful.

Evaluation of the activation energy trend as a function of  $\chi_1$  (Figure 6c) clearly discloses that the CPI, CBQ, and CNA reacting moieties as alkylating agents toward ammonia are activated by the rotation of the NH<sub>2</sub> group up to  $\chi_1 = 120^\circ$ , not only in gas phase but also in polar bulks. Although the extent of such an activation from 0° to 120° reaches its maximum in gas phase with a value of –8.4 kcal mol<sup>-1</sup>, the reduction of the reaction activation energy is strongly operative also in solvent bulk. In fact, the maximum conformational catalytic effect on the activation energy of the reaction is –4.1 and –4.3 kcal mol<sup>-1</sup> in acetonitrile and water, respectively. Although on passing from gas to condensed phase the activation of the alkylating unit maintains an important contribution from the conformational catalysis (about –4 kcal mol<sup>-1</sup>), the major contribution to the reactivity enhancement (15–18 kcal mol<sup>-1</sup>) comes from the stabilization of the zwitterionic TS by the electrostatic component of the solvent bulk.

**2.2. Conformational Effects on Activation of the N<sub>10</sub>-Formyl Derivatives.** We have so far computationally supported the existence of a conformational catalysis in gas phase and in polar solvent bulk induced by twisting the  $\chi_1$  dihedral angle. An alternative possibility for inducing conformationally triggered change in the energetics of the alkylation reaction involves a rotation of the formyl group around the N<sub>10</sub>–C<sub>11</sub> bond (i.e., by variation of the  $\chi_2$  dihedral angle, in Scheme 5, that gradually transforms the substrate **9Z** and TS **S9Z** into **9E** and **S9E**, respectively). In fact, such a conformational mobility of the amide group should reduce the electron-withdrawing effect of the formyl group on both reactant and TS and could cause a change in the reaction activation energy, if the extent of the amide conjugation effect in the reactant **9** is not comparable to that of TS **S9**. Such

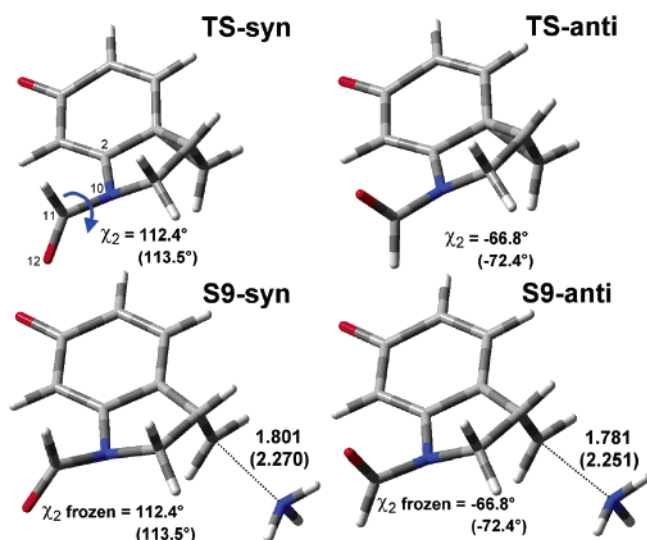


**FIGURE 8.** Conformational TSs **TS-syn** and **TS-anti** for the interconversion of the two conformers **9Z** and **9E** and  $\chi_2$  locked TSs **S9-syn** and **S9-anti**.  $\chi_2$  angle values and forming bond distances are reported at the B3LYP/6-31+G(d,p) level in gas phase and in water (in parentheses).

**TABLE 6.** Relative Energies (kcal mol<sup>-1</sup>)<sup>a</sup> of TSs Governing Rotation of the Formyl Group around the N<sub>10</sub>-C<sub>11</sub> Bond in Reactant **9** at the B3LYP Level with Different Basis Sets, in Gas Phase and in Water Solution (in Parentheses)

structure	6-31G(d)	6-31+G(d,p)
<b>TS-syn</b>	18.7 (18.5)	18.5 (18.2)
<b>TS-anti</b>	19.5 (19.7)	19.6 (19.8)

<sup>a</sup> Relative to the most stable minimum **9E**. **9Z** is less stable than **9E** by 2.1 (0.6) and by 2.4 (0.9) with 6-31G(d) and 6-31G+(d,p) basis sets, respectively.

a conformational distortion could be partially induced by the binding of the substrate to DNA and can be simulated computationally to the limit situation when the formyl group and nitrogen lone pair are coplanar. We started such a conformational analysis, locating the TSs **TS-syn** and **TS-anti** (Figure 8) for the interconversion of the two minima **9Z** and **9E** with the formyl oxygen *syn* and *anti*, respectively, to the cyclopropane ring undergoing opening.

Geometries and activation energies have been computed with and without diffuse functions [6-31G+(d,p) and 6-31G(d)] also in gas phase and in water solution without any meaningful differences (Table 6).

Data in Table 6 allow a quantitative evaluation of the formyl rotational barrier around the N<sub>10</sub>-C<sub>11</sub> bond, both in gas phase and in water solution, which is almost identical to the experimental rotational barrier of the formamide.<sup>41</sup> These conformational TSs displays a strongly pyramidalized nitrogen in both cases with the lone pair *syn* to the cyclopropane methylene group and coplanar to the formyl HC<sub>11</sub>(O) moiety (Figure 8). These data suggests that the complete loss of the N<sub>10</sub>-C<sub>11</sub>(O) amide conjugation in **9** destabilizes the reactant slightly more than 18 kcal mol<sup>-1</sup>.

To evaluate how much an analogue loss of the N<sub>10</sub>-C<sub>11</sub>(O) amide conjugation will raise the energy of the TS, we located **S9-syn** and **S9-anti** TSs (Figure 8) locking

the geometry of the N<sub>10</sub>-C<sub>11</sub>(O) amide to that of the stationary points **TS-syn** and **TS-anti**. The structure **S9-syn** [with a C-N forming bond slightly shorter (1.801 Å) than that of the real TS **S9E** (1.827), in gas phase with 6-31+G(d,p) basis sets] displays the formyl oxygen atom *syn* to the cyclopropane methylene group undergoing ring opening and is more stable than **S9-anti** by 3.0 kcal mol<sup>-1</sup> in gas phase and 2.2 kcal mol<sup>-1</sup> in water. The energy of **S9-syn** is 20.8 kcal mol<sup>-1</sup> higher than that of the real TS **S9E**. In other words the loss of the N<sub>10</sub>-C<sub>11</sub>(O) amide conjugation destabilizes the TS (+20.8 kcal mol<sup>-1</sup>) more than the reactant **9E** (+18.7 kcal mol<sup>-1</sup>), in gas phase. Similar results have been obtained in water solution where the loss of the N<sub>10</sub>-C<sub>11</sub>(O) amide conjugation destabilizes the TS more than the reactant **9E** by 1.6 kcal mol<sup>-1</sup>.

These data suggest that the formyl group acts as a selective TS stabilizing substituent (in comparison to the reactant), through its electron-withdrawing property that lessens the destabilizing effect of the NH<sub>2</sub> on the developing negative charge on the cyclopropylcyclohexadienone moiety in the TS.

In addition, the data display that the rotation of the formyl group is unlikely to cause a conformational catalysis for two reasons: (i) the torsion of the  $\chi_2$  dihedral angle in the reactants is energetically demanding, requiring ~18 kcal mol<sup>-1</sup>, and (ii) above all such a conformational change actually causes a slight deactivation of the CPI moiety, both in gas phase and in water solution.

## Conclusion

Our study, computing the activation energy for the ammonia alkylation reaction by several substrates optimized both in gas phase and in water solution [at B3LYP and B3LYP-C-PCM level of theory, with 6-31G(d) and 6-31+G(d,p) basis sets], quantitatively evaluates the role of several structural key features of the CPI reactive subunit as alkylating agent in the uncatalyzed addition of ammonia. Our computational results indicate a strong enhancement of the electrophilicity of CPI due to the *N*-formyl substitution, as a result of the stabilizing effect of the formyl group in the TS. We have also been able to quantify the effect of the vinylogous stabilization of the reactants (by -6.1 and -10.7 kcal mol<sup>-1</sup> in gas phase and in water, respectively) and of a condensed pyrrole ring (which reduces the CPI reactivity, rising the activation energy by +8.9 kcal mol<sup>-1</sup>). Both of these effects reduce the reaction rates. However, in our opinion, the most worthy result of this computational investigation is the quantitative evaluation of the conformational effects of NH and *N*-formyl moieties (described by  $\chi_1$  and  $\chi_2$  dihedral angles, respectively) of the CPI subunit on the activation energy of the ammonia alkylation. The enhancement of CPI reactivity as a consequence of the conformational mobility is strong in gas phase, since the flexibility of  $\chi_1$  dihedral angle causes a drop of -8.4 kcal mol<sup>-1</sup>. This finding provides for the first time computational evidence of a conformational catalysis. Conformational catalysis induced by variation of the  $\chi_1$  dihedral angle remains significant in water solution (-4.3 kcal mol<sup>-1</sup>). Furthermore the loss of the N<sub>10</sub>-C<sub>11</sub>(O) amide conjugation, through the raising of the  $\chi_2$  dihedral angle values, causes a slight conformational deactivation of the CPI reactivity both in gas phase and in water solution.

From a methodological point of view this study supports the importance of a computational approach in the evaluation of the “conformational catalysis” of an important class of alkylating agents in a polar bulk. In addition it highlights the necessity of taking into account the conformational effects on the energies of both reactants and TSs. Work is still in progress to address the important issue of the conformational catalysis on models more similar to CPIs.

**Acknowledgment.** Financial support from Pavia University (“Fondo FAR 2002”) is gratefully acknowl-

edged. We also thank CICAIA (Modena University) and CINECA (Bologna University) for computer facilities.

**Supporting Information Available:** Energies and Cartesian coordinates of stationary points in Figures 1–5, 7, and 8 in the gas phase and in water solution, optimized at B3LYP with 6-31G(d) and 6-31+G(d,p) level of theory. This material is available free of charge via the Internet at <http://pubs.acs.org>.

JO049193P